# Achievements of strong motion seismology in 20th century and its future directions

Kojiro Irikura
Disaster Prevention Research Institute, Kyoto University, Uji, Kyoto 611-0011

## ABSTRACT

We have been trying to make a recipe for predicting ground motions from future large earthquakes. To do that the most important factors are the source characterizations for complex rupture processes and the Green's function estimations for realistic geological structures. We attempt to formulate the source characterizations based on recent results of the waveform source inversion. There are two important aspects of characterizing the earthquake sources, outer and inner source parameters. The outer source parameters such as total fault length, width, seismic moment and so on are obtainable based on geological investigations of capable earthquake faults and seismological studies of source models. The inner source parameters are parameters related to slip heterogeneity on fault plane from the waveform inversion of strong motion records. We find that the areas of large slip known as asperities follow a self-similar scaling as well as the total rupture areas from the statistical analysis of the inverted results. This implies that both parameters, outer and inner ones, are predictable. Based on the results above mentioned we construct the procedure of characterizing the source for scenario earthquakes compiling accumulated knowledge about earthquake faults in geomorphology and seismology. We have examined the procedure comparing between observed records and synthetic ground motions from the characterized sources based on kinematic models for the recent large earthquakes. Then, we have confirmed the validity of the procedures for characterizing the earthquake sources and calculating ground motions. In future directions, the validity and applicability of predicting strong ground motions should be made taking into account source dynamics physically realizable. For example, surface displacements for the above model should be estimated from dynamic rupture process, assuming additional source parameters such as critical slip and strength excess for dynamic source simulation and compared with observed ones from geological and geomorphological survey.

## INTRODUCTION

Recent large earthquakes, such as the 1995 Kobe (Japan) earthqauke, the 1999 Kacaeli (Turkey) earthquake, and the 1999 Chi-chi (Taiwan) earthquake occurred on well-mapped active faults. However, no obvious precursory evidences appeared even near the faults before the events. On the other hand, high-quality ground motion records have been obtained from those recent earthquakes.

Accumulated data have been providing us very important knowledge about rupture processes of earthquakes, propagation-path and site effects on ground motion, the relation between ground motion and damage, and so on. Then, we have learned that earthquake damage resulted from destructive ground motion generated by rupture propagation effects in asperities as well as geological conditions.
For example, heavy damage in Kobe area larger than in the Awaji area during the 1995 Hyogo-ken Nanbu earthquake is explained by source effects such as slip heterogeneity and forward rupture directivity and basin-edge effects due to basin structures. In the Awaji area there was less damage although surface breaks appeared along the Nojima faults. This means the importance of strong ground motion prediction from earthquake faults to mitigate disaster for future earthquakes.

Scenario earthquakes for subject areas have gradually been popular to make seismic disaster prevention measures by some governmental agencies and municipalities. However, most of strong motion estimations in earthquake hazard analysis are still inclined to empirical methods. Peak ground acceleration and velocity and response spectrum for earthquake-resistant design are given by empirical methods as a function of magnitude, fault distance, ground condition. They have not been taken into account yet developments in seismology, such as source processes in earthquake faults and 3-D simulation in complex structures.

We made a framework of strong motion prediction as shown in Fig. 1. The strong motion from the scenario earthquake is evaluated from source modeling and Green's function estimation based on geological and geomorphological survey of active faults, geophysical profiling of underground structures, strong motion recordings, and so on. The results will lead to improvement of the building code and bridge earthquake-resistant design.

## RECIPE FOR STRONG MOTION PREDICTION

We attempted to make a recipe to popularize the prediction of ground motions for engineering purpose based on seismological fruits. There are two important factors for predicting strong ground motion, one is source characterization based on geological features for active faults and statistical analysis of source processes from the waveform inversion of strong motion records, the other is the estimation of the Green's functions from source to site.

For the former, we know that most of the uncertainties in predicting strong ground motion is to specify the proper methods of characterizing the source models of future earthquakes. Conventional source parameters such as fault length and width and average slip on fault are only available for very long period motions but not enough for near-source strong motions dominating short period motions less than 1 sec of engineering interest. Slip heterogeneity on the fault plane plays important role on such short period motions. We tried to make source characterization including slip heterogeneity based on the statistical analysis of the source inversion results.

For latter, numerical Green's functions are calculated for ground motions longer than 1sec based on methods such as Discrete Wave Number Method, Finite Deference Method, and Finite element method. The short period motions are estimated by the empirical Green functions and stochastic simulation method for small events. To combine the long and short period motions, introduce the idea of a hybrid method estimating the Green's functions, deterministic and stochastic approaches in low (< 1 Hz) and high (> 1 Hz) frequency ranges, respectively, to obtain broad-band ground motions (Irikura and Kamae, 1999).

For estimating strong ground motions in a deterministic approach, we need to have two kinds of source parameters, outer and inner ones.

**Outer Source Parameters**

The outer source parameters are total fault length and width, average slip and slip duration, rupture velocity and so on, which are to characterize the macroscopic pictures of given source faults. They are inferred, based on geological investigations of capable earthquake faults and seismological studies of source models.

**Total fault lengths (*L*)** of scenario earthquakes would be evaluated as one of the long-term seismic hazard evaluation. Some attempts have been making to estimate segmentation and grouping of active faults based on branching features of seismic surface ruptures (e.g. Matsuda, 1998; Nakada, 1998). Such surveys give us **strike ($\phi$)** and **slip type** of every segment consisting of the fault system. **Dip angle ($\delta$)** is inferred from seismic reflection profile.

**Fault width (*W*)** cannot be directly determined from the geological survey but mostly from source modeling for waveform simulations compared with observed records. The saturation of the width yields for events larger than M6.8, corresponding the thickness of seismogenic zones. The seismogenic zones are infered from the depth-frequency distribution of small earthquakes (Ito, 1990).

Recent study by Ito (1999) shows that the seismogenic zones seem to have upper cutoff depth as well as lower cutoff depth derived from the seimic-aseismic boundary in the mid-crust dependent on regions.

The **seismic moment** of the capable faults are estimated by the empirical relationship between the source areas and seismic source(A = LW), then average slips are automatically constrained by the seismic moment and source area (e.g. Somerville et al. 1999).

**Inner Source Parameters – Fault Heterogeneity or Roughness –**

The slip and slip velocity have been found not to be uniform in the source areas, in particular for large earthquakes more than 7 as clarified from the waveform inversion of rupture process (e.g. Wald, 1996). We need to know slip and slip velocity distribution in the source area as well as the average slip to estimate strong ground motions. We call here such source parameters inner source parameters that express fault heterogeneity or roughness. So far slip models have been derived from longer period ground motions using the waveform inversion. Direct application of such long-period source models to strong ground motion estimation is not always available because higher ground motions than 1 Hz cannot be generated. Nevertheless, we found that the asperity models derived from the heterogeneous slip distribution using the waveform inversion of longer-period ground-motion recordings are available for estimating broad-band ground motions of engineering interest (e.g. Kamae and Irikura, 1998).

Somerville et al. (1999) analyzed the characteristics of slip models of totally fifteen crustal earthquakes ranging from about 6 to 7 in moment magnitude (Mw) for use in the prediction of strong ground motion. They used two approaches, deterministic and stochastic, in characterizing the slip models. First they define **fault asperities** in a deterministic manner to quantify the properties of heterogeneous slip models. The asperities are areas on the fault rupture surface that have large slip relative to the average slip on the fault. An asperity is defined to enclose fault elements whose slip is 1.5 or more times larger than the average slip in the fault (in detail refer to Somerville et al.,1999). The number of asperities in the slip models of those events is 2.6 on average. The slip contrast, the average slip on the asperities over average slip is about 2. The combined area of asperities on average occupies about 22% of the total rupture area.

Total rupture area (A), combined area of asperities (Aa), and area of largest asperity (Am) scale in a self-similar manner with increasing seismic moment.

$$A(km^2) = 2.23 \times 10^{-15} \times Mo^{2/3}(dyne\text{-}cm) \qquad (1)$$

$$Aa(km^2) = 5.00 \times 10^{-16} \times Mo^{2/3}(dyne\text{-}cm) \qquad (2)$$

$$Am(km^2) = 3.64 \times 10^{-16} \times Mo^{2/3}(dyne\text{-}cm) \qquad (3)$$

The validity and applicability of estimating strong ground motion based on the above recipe should be examined in comparison with the simulated motions and observed records.

## SIMULATION OF STRONG GROUND MOTION FROM THE 1999 KOCAELI EARTHQUAKE

Strong ground motions from the 1999 Kocaeli earthquake were recorded near the causative faults as shown in lower panel of Fig. 2. We characterize the source model with asperities based on the slip distribution (Upper panel of Fig.2) determined from the inversion of strong motion data by Sekiguchi and Iwata (2000). The ground motions from the mainshock are estimated using the hybrid method (Irikura and Kamae, 1999). We assume pure right-lateral strike slip at each asperity. The size of the subfaults generating the small events is assumed to be 2x2 $km^2$. For simplicity, we take into account each asperity as a event with uniform stress drop in a finite extent. The best fit model to observed records is composed of three asperities (three small rectangles in the upper panel of Fig. 2). The stress drop ($\Delta\sigma$) in each asperity is assumed to be 120 bars in Asperity 1, 50 bars in Asperity 2 and 100 bars in Asperity 3, assuming circular crack (Brune, 1970). Rupture was initiated at the corner of each asperity. The synthesized motions, acceleration and velocity and the acceleration response spectra are compared with the observed at SKR (close to the surface rupture about 40 km east of epicenter, see Fig.2) and GBZ (about 50 km west of epicenter) in Fig. 3 and 4. At SKR, only EW-component was recorded. Slips are assumed to exist only on those three asperities and no slips in the background areas. The synthetic velocity motions agree well with the observed ones in phase, although they seem to be a little less than the observed ones, while the synthetic acceleration are almost the same amplitude as the observed. Total seismic moment obtained from the synthetic motions are assumed to be 44% of the observed ones because zero slips are assumed on the background area. It is why the synthetic velocity motions are a little less.

## SIMULATION OF STRONG GROUND MOTION FROM THE 1999 CHI-CHI EARTHQUAKE

We assume an initial source model consisting of three asperities based on the results of the kinematic waveform inversion (Iwata et al., 2000), a large asperity No.3 in the northern part of the causative fault and two smaller asperities No.1 and No.2 in southern part near the epicentral area as shown in Fig. 5. We used the same hybrid method for simulating ground motion as the above. We assumed a rake angle of $60^{o}$ for the subfaults of the asperities No1 and No.2 in the southern part and a rake angle of $45^{o}$ for those of the asperity No.3 in the northern part. We assume that the surface layers with total thickness of 3 km do not generate high frequency motions following the idea of the dynamic rupture process (Dalguer et al., 2001).

The best-fit source model between the observed and synthetic motions is as follows. The stress drop is assumed to be 100 bars at those three asperities. The rise time for each asperity is taken to be 0.6 sec. The synthetic motions are compared with the observed ones at TCU078, one of the sites at the southern part near the epicenter in Fig. 6 and at TCU046 one of the sites at the north of the Chelumpu fault in Fig. 7. We find that the acceleration and velocity waveform and the acceleration response spectra of the synthetic motions at both stations show good agreement with those of the observed ones, although the characteristics of the waveforms are very different each other at those two stations. The waveforms at TCU078 close to the epicenter is composed of high-frequency and long duration wavelets. It comes from the fact that this site is located in the backward direction of those three asperities.

The velocity motions synthesized here as well as those observed at TCU045 are composed of a single large pulse with duration of about 10 sec. This pulse is indicative of the forward rupture directivity due to a large asperity of No.3, because the rupture propagated from south to north to break Asperity No. 3 north of the hypocenter. Similar large pulses in the near-source area were observed during the 1992 Landers earthquake in California, USA and the 1995 Hyogo-ken Nanbu earthquake. The predominant periods of the near-source pulses in forward rupture direction depends on the asperity size and slip duration (Irikura et al., 1996; Somerville et al, 1996).

## SCALING RELATIONS BETWEEN ASPERITY AREAS AND SEISMIC MOMENT

The relation between the combined area asperities and seismic moment and that between the area of the largest asperities and seismic moment are compiled in Fig. 8. Adding fifteen crustal earthquakes analyzed by Somerville et al.(1999), there were plotted three crustal earthquakes in Japan by Miyakoshi et al.(2000), and the 1995 Kobe, the 1999 Kocaeli, the 1999 Chi-Chi, and 2000 Tottori earthquakes by Sekiguchi and Iwata (2000) and by Iwata and Sekiguchi (2000). The maximum seismic moment analyzed by Somerville et al.(1999) is $75 \times 10^{25}$ dyne-cm. Newly analyzed results shows the self-similar scaling relations by them can be extended to larger earthquake. We do not know the saturation levels of those relations yet.

The combined area of asperities and the area of the largest asperities obtained from the best-fit models in this study are also shown by squares with cross mark in the same figures. We find that the results for the 1994 Northridge, 1995 Kobe, 1999 Kcaeli, and 1999 Chi-Chi earthquake almost follow the self-similar scaring relationship.

## CONCLUSION

We summarized the procedure for predicting strong ground motions from future earthquakes caused by inland active faults as a recipe. The source characterization for the future earthquakes are made by the statistical analysis of the source inversion using strong motion and teleseismic data. Adding fifteen crustal earthquakes analyzed by Somerville et al.(1999), more results are compiled, three crustal earthquakes in Japan by Miyakoshi et al.(2000), and the 1995 Kobe, the 1999 Kocaeli, the 1999 Chi-Chi, and 2000 Tottori earthquakes by Sekiguchi and Iwata (2000) and by Iwata and Sekiguchi (2000). Then, we find that the combined area of asperities and the areas of the largest asperity as well as total rupture area follows the self-similar scaling. The seismic moment range applicable are extended to $2.75 \times 10^{27}$ dyne-cm (Mw 7.6).

The validity and applicability of the source characterization for strong ground prediction are examined in comparison with the observed records and broad-band simulated motions using the hybrid mehtod from recent large earthquakes such as the 1995 Hyogo-ken Nanbu (Kobe) earthquake, the 1994 Northridge earthquake, 1999 Kacaeli earthquake, 1999 Chi-Chi earthquake.

In future directions, strong ground motions should be made taking into account source dynamics physically realizable. Observed surface displacements from geological and geomorphological survey should be compared with simulated ones taking into account from dynamic rupture process, additional source parameters such as critical slip and strength excess for dynamic theory.

**Acknowledgement**

This paper was made by cooperation with Tomotaka Iwata, Katsuhiro Kame, Takao Kagawa, Ken Miyakoshi, and Hiroe Miyake. Figures are arranged by Hiroe Miyake getting analyzed results from the co-researchers above mentioned. This study was partially supported by a grant-in-Aid for Scientific Research, Number 09044079, from the Ministry of Education, Science, Sports, and Culture.

## REFERENCES


Dalguer, L. A., K. Irikura, J. D. Riera, and H. C. Chiu (2001), “Fault dynamic rupture simulation of the hypocenter area of the thrust fault of the 1999 Chi-Chi (Taiwan) earthquake”, *Geophys. Res. Letter*, 27, in press.

Irikura and Kamae (1999), “Strong ground motions during the 1948 Fukui earthquake”, *Zisin (J. Seism. Soc. Japan)*, 52, pp129-150 (in Japanese).

Irikura, K., T. Iwata, H. Sekiguchi, A. Pitarka, and K. Kamae, Lesson from the 1995 Hyogo-ken Nanbu earthquake: Why were such destructive motions generated to buildings ?, J. Natur. Disas. Sci., 18, 99-127, 1996.

Ito, K. (1990), “Regional variations of the cutoff depth of seismicity in the crust and their relation to heat flow and large inland-earthquakes”, *J. Phys. Earth.*, 38, pp223-250.

Ito, K. (1999), “Seismogenic layer, reflective lower crust, surface heat flow and large inland-earthquakes”, *Tectonophysics*, 306, pp423-433.

Iwata, T., H. Sekiguchi, and K. Irikura, 2000, Rupture process of the 1999 Chi-Chi, Taiwan, earthquake and its near-source strong ground motions, Proc. International Workshop on Annual Commemoration of Chi-Chi earthquake, Taipei, Taiwan, 1, 36-46.

Kamae, K. and K. Irikura (1998), “Source model of the 1995 Hyogo-ken Nanbu earthquake and simulation of near-source ground motion”, *Bull. Seism. Soc. Am.* , 88, pp400-412.

Matsuda, T. (1998), “Present state of long-term prediction of earthquakes based on active fault data in Japan, *Zisin (J. Seism. Soc. Japan)*, 50, pp23-34 (in Japanese).

Miyakoshi, K., T. Kagawa, H. Sekiguchi, T. Iwata, and K. Irikura, 2000, Source characterization of inland earthquakes in Japan using source inversion results, *Proc. 12WCEE* (CD Rom), 3, 1850.

Nakata, T., K. Shimazaki, Y. Suzuki, and E. Tsukuda (1998), “Fault branching and directivity of rupture propagation”, *Journal of Geography*, 107, pp512-528 (in Japanese).

Sekiguchi, H., K. Irikura, and T. Iwata, 2000, Fault geometry at the rupture termination of the 1995 Hyogo-ken Nanbu earthquake, *Bull. Seism. Soc. Am.*, 90, 974-1002.

Sekiguchi, H. and T. Iwata, 2000, Rupture process of the 1999 Kocaeli, Turkey, earthquake using strong motion waveforms, submitted to *Bull. Seism.Soc. Am*.

Somerville, P., K. Irikura, R. Graves, S. Sawada, D.Wald, N. Abrahamson, Y. Iwasaki, T. Kagawa, N. Smith, and A. Kowada (1998), “Characterizing earthquake slip models for the prediction of strong ground motion”, *Seismological Research Letters*, 70, pp59-80.

Wald, D. J. (1996), “Slip history of the 1995 Kobe, Japan, earthquake determined from strong motion, teleseismic, and geodetic data”, J. Phys. Earth, 44, pp489-503.

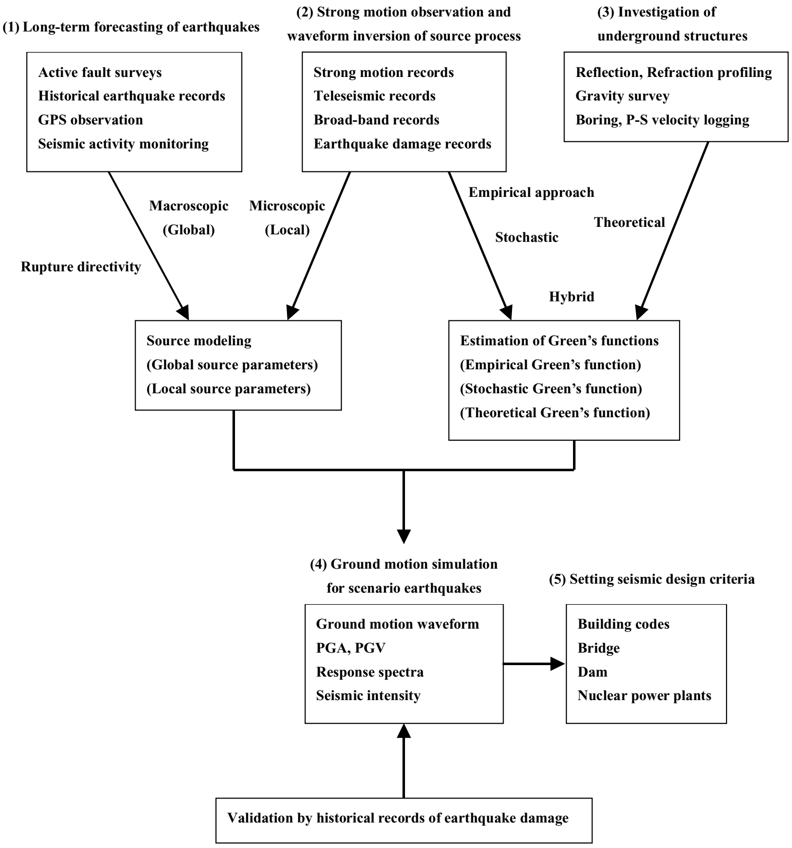


Fig. 1. Framework of predicting strong ground motion from scenario earthquake.

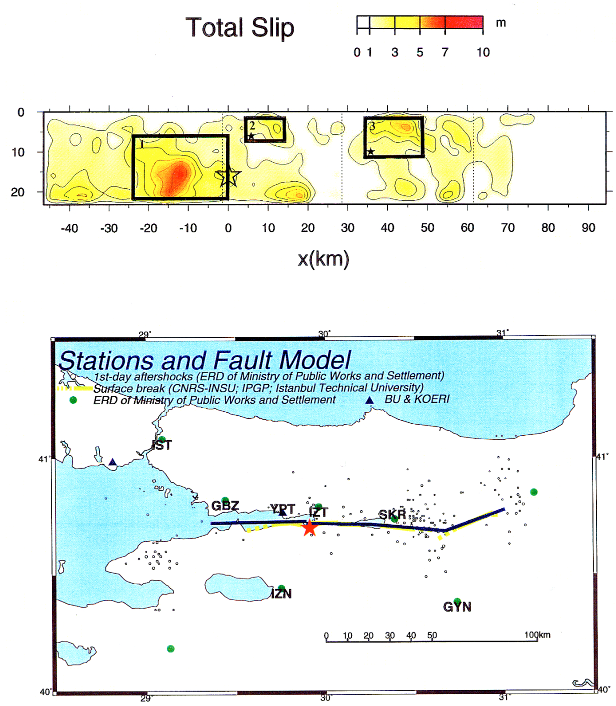


Fig. 2. Upper: Slip distribution derived from the waveform inversion by Sekiguchi and Iwata (2000) and characterized source model composed of three asperities for the 1999 Kocaeli earthquake. Lower: Map of the surface fault trace inferred for the source inversion and strong motion stations.

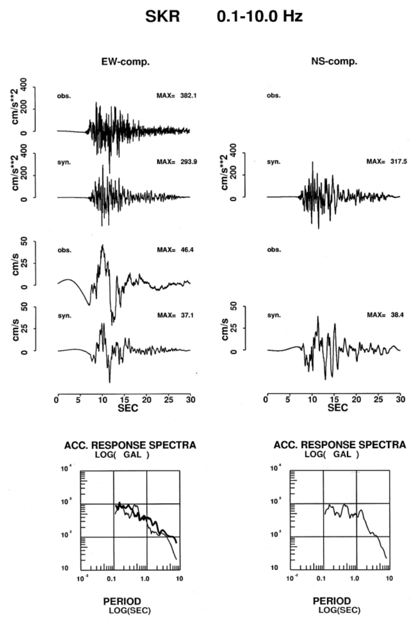


Fig. 3. Comparison between the synthetic acceleration and velocity seismograms and their acceleration response spectra of EW component close to fault normal using the hybrid method and observed ones at SKR. The acceleration and velocity seismograms NS component close to fault parallel are simulated with the same model, although it failed in recording. This station is located close to the surface rupture about 40 km east of epicenter.

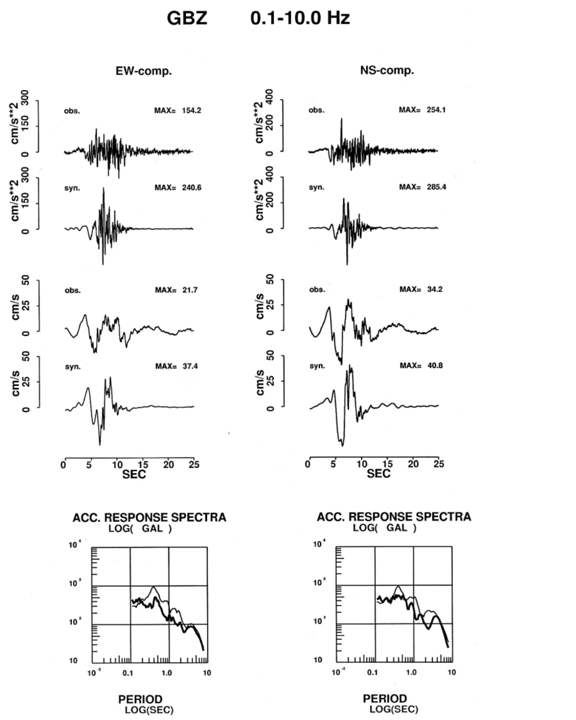


Fig. 4. Comparison between the synthetic acceleration and velocity seismograms (EW component close to fault normal and NS component close to fault parallel) and their acceleration response spectra of using the hybrid method and observed ones at GBZ. This station is located close to the surface rupture about 50 km west of epicenter.

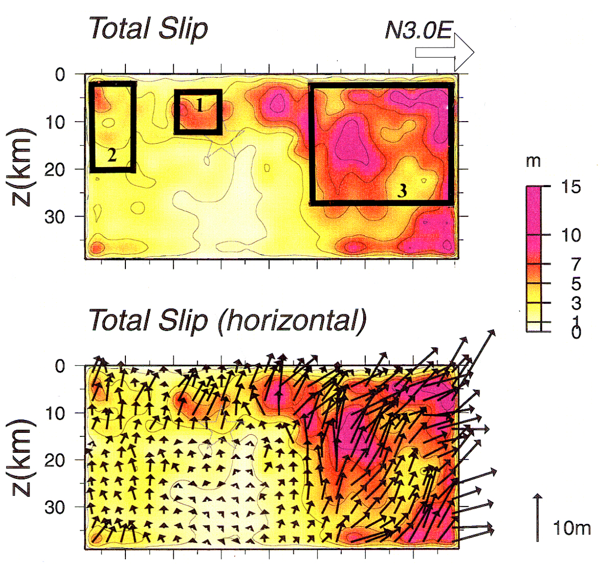


Fig. 5. Slip distribution with slip vectors (Lower) from the waveform inversion by Iwata et al. (2000) and characterized source model with three asperities (Upper) for the 1999 Chi-chi earthquake.

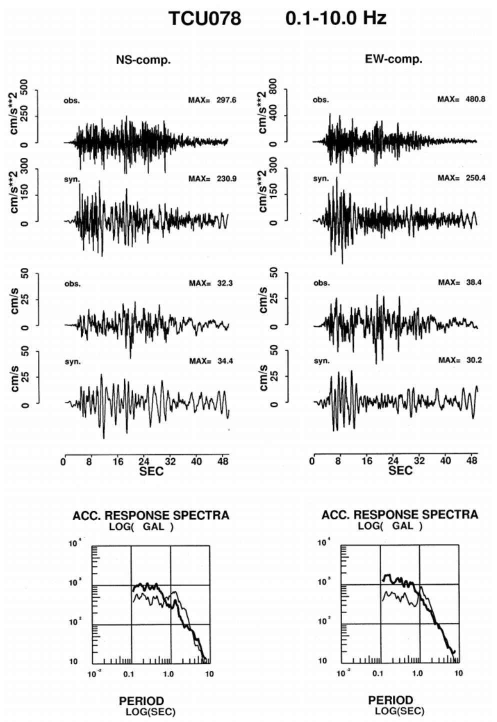


Fig. 6. Comparison between the synthetic acceleration and velocity seismograms (EW component close to fault normal, NS component close to fault parallel) and their acceleration response spectra using the hybrid method and observed ones at TCU078. This station is located close to the epicenter at the southern part of the causative fault.

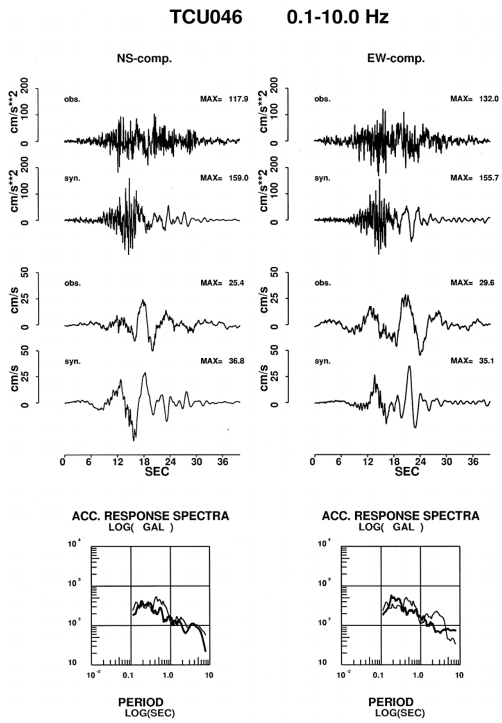


Fig. 7. Comparison between the synthetic acceleration and velocity seismograms (EW component close to fault normal, NS component close to fault parallel) and acceleration response spectra using the hybrid method and observed ones at TCU046. This station is located northern part of the causative fault.

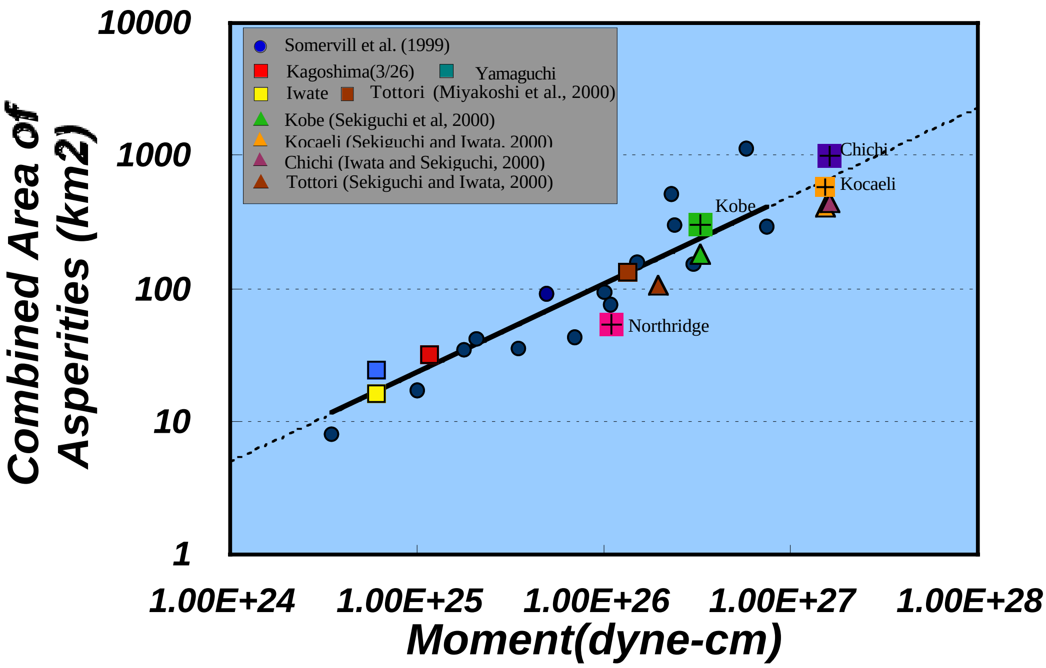


Fig. 8. Relation between combined area of asperities and seismic moment based on slip distributions estimated by the waveform inversion by Somervillle et al. (1999), Miyakoshi et al. (2000), Sekiguchi et al. (2000), Sekiguchi and Iwata (2000), and Iwata and Sekiguchi (2000). The individual events analyzed are listed at the left-upper corner panel. The line is a least-squares fit under the constraint of self-similarity (slope=2/3) by Somervillle et al. (1999). The combined asperity areas determined from comparison between the synthetic and observed waveforms in this study are plotted by squares with cross.

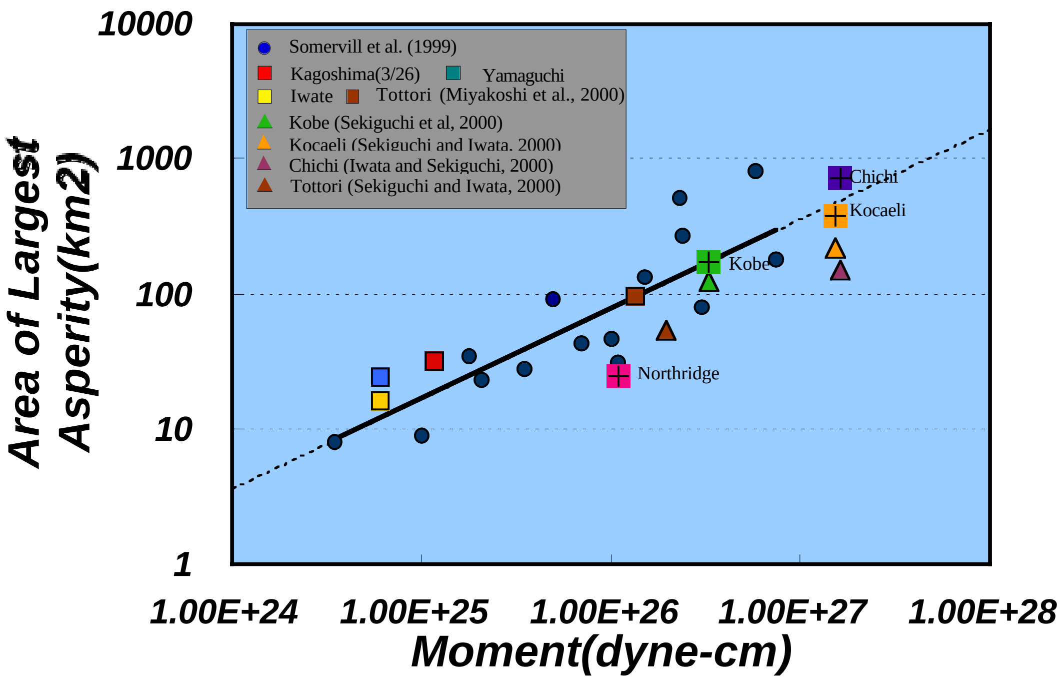


Fig. 9. Relation between area of largest asperity and seismic moment based on slip distributions estimated by the waveform inversion. The data sources are the same a Fig. 8. The line is a least-squares fit under the constraint of self-similarity (slope=2/3) by Somervillle et al. (1999). The largest asperity areas determined from comparison between the synthetic and observed waveforms in this study are plotted by squares with cross.